

# Correlations between the fragmentation modes and light charged particles emission

Yingxun Zhang<sup>a,\*</sup>, Chengshuang Zhou<sup>a,b</sup>, Jixian Chen<sup>a,b</sup>, Ning Wang<sup>b</sup>, Kai Zhao<sup>a</sup>, Zhuxia Li<sup>a</sup>

<sup>a</sup>China Institute of Atomic Energy, P.O. Box 275 (10), Beijing 102413, P.R. China

<sup>b</sup>College of Physics and Technology, Guangxi Normal University, Guilin 541004, P.R. China

---

## Abstract

The correlations between the shape of rapidity distribution of the yield of light charged particles and the fragmentation modes in semi-peripheral collisions for  $^{70}\text{Zn}+^{70}\text{Zn}$ ,  $^{64}\text{Zn}+^{64}\text{Zn}$  and  $^{64}\text{Ni}+^{64}\text{Ni}$  at the beam energy of 35MeV/nucleon are investigated based on ImQMD05 code. Our studies show there is interplay between the binary, ternary and multi-fragmentation break-up modes. The binary and ternary break-up modes more prefer to emit light charged particles at middle rapidity and give larger values of  $R_{yield}^{mid}$  compared with the multi-fragmentation break-up mode does. The reduced rapidity distribution for the normalized yields of p, d, t,  $^3\text{He}$ ,  $^4\text{He}$  and  $^6\text{He}$  and the corresponding values of  $R_{yield}^{mid}$  can be used to estimate the probability of multi-fragmentation break-up modes. By comparing to experimental data, our results illustrate that  $\geq 40\%$  of the collisions events belong to the multi-fragmentation break-up mode for the reaction we studied.

*Keywords:* fragmentation modes, emission of light charged particles, symmetry energy

---

Fragmentation mechanism, i.e. does a nucleus break up into several intermediate mass fragments (IMFs) in intermediate energy heavy ion collisions (HICs) in a statistical (thermal) way or dynamical way, has been a long-standing problem in nuclear physics, and it has attracted a lot of theoretical

---

\*Corresponding author

*Email address:* zhyx@ciae.ac.cn (Yingxun Zhang)

and experimental efforts. Up to now, both the statistical and dynamical approaches can equally well describe many observables in intermediate energy HICs, such as charge distributions, mean kinetic energies of the emitted fragments and so on, but each of them fail to describe some observables predicted by others, such as the isotope yields, isoscaling, isospin diffusion, bimodality [1, 2, 3, 4, 5, 6, 7, 8, 9, 10, 11, 12, 13, 14]. It turns out that this problem is still open and the situation is very complicated. One may not simply attribute the fragmentation mechanism to dynamical or statistical way, and both approaches may be complement each other for low-intermediate energy heavy ion collisions.

Previous study in reference[15] has shown there is interplay between the binary/ternary break-up (fusion-fission) modes and multi-fragmentation mode, especially for the low-intermediate energy HICs (20-40MeV/nucleon). The binary and ternary break-up [13, 14, 15, 16, 17, 18, 19] modes are mainly related to a slow process[20, 21] which can also be described in the statistical way, and multi-fragmentation break-up mode is related to a fast process which can be described in dynamical way. Special attentions have been paid to semi-peripheral collisions at low-intermediate energy for further understanding the fragmentation mechanism, because it is the best way to study the interplay between fusion-fission and multi-fragmentation [17, 18, 19, 22, 23, 29, 24, 25] process. In experiment, Kohley et al studied the semi-peripheral collisions of  $^{70}\text{Zn}+^{70}\text{Zn}$ ,  $^{64}\text{Zn}+^{64}\text{Zn}$ , and  $^{64}\text{Ni}+^{64}\text{Ni}$  at the beam energy of 35MeV/nucleon[24]. The data of rapidity distributions for normalized yields of isotopically light charged particles (LCPs), i.e.  $Y(y_r)/Y(y_r = 0)$ , of p, d, t,  $^3\text{He}$ ,  $^4\text{He}$  and  $^6\text{He}$ , are reported. Those data show a clear preference for emission around the middle rapidity region ( $|y_r| < 0.5$ , where  $y_r = \frac{y_{c.m.}}{y_{proj}}$ ), especially for more neutron-rich LCPs due to the isospin drift and diffusion[26, 29]. However, the experimental results on the reduced rapidity distributions of the normalized yields of proton and  $^3\text{He}$  tend to have an increased forward rapidity yield relative to the Stochastic Mean Field model(SMF)[27, 28] calculations with both soft and stiff symmetry energy cases. Those discrepancies could be attributed to the decay of quasi-projectile (QP) at later stages of the reaction [24]. Recent studies for  $^{124}\text{Sn}+^{64}\text{Ni}$  show that the parallel velocity distribution for the yields of  $Z=3-6$  fragments can be described after coupling the sequential decay to the transport models[32], but there still have little differences between data and theory. It seems to us that the statistical decay is not enough to explain the

discrepancy on the rapidity distribution of LCPs between theory and experiment, and we still need to understand it in the dynamical approaches besides sequential decay. By the way, the symmetry energy play important roles in determination of the isotope distribution of emitted fragments in transport model because its values directly related to the thickness of neutron skin and the borderline of nuclear chart[33, 34, 35] in theoretical prediction.

In this paper, we investigate the dynamical correlations between the fragmentation modes and LCPs emission by analyzing the rapidity distributions of the yields for LCPs and the branching ratio of different break-up mode for semi-peripheral collisions of  $^{70}\text{Zn}+^{70}\text{Zn}$ ,  $^{64}\text{Zn}+^{64}\text{Zn}$ , and  $^{64}\text{Ni}+^{64}\text{Ni}$  at the beam energy of 35MeV/nucleon by using ImQMD05 code. The influence of different impact parameters and symmetry energy are also discussed. Since the main goal of this work is to investigate the correlation between the fragmentation modes and LCPs emission, there is no attempt to obtain the best fit to the data.

Within the ImQMD05, nucleons are represented by Gaussian wavepackets and the nucleonic mean fields acting these wavepackets are derived from an energy density functional. The potential energy  $U$  that includes the full Skyrme potential energy with just the spin-orbit term omitted and the Coulomb energy reads as:

$$U = U_{\rho,md} + U_{coul}. \quad (1)$$

The nuclear contributions are represented in a local form with

$$U_{\rho,md} = \int u_{\rho,md} d^3r \quad (2)$$

and

$$\begin{aligned} u_{\rho} = & \frac{\alpha}{2} \frac{\rho^2}{\rho_0} + \frac{\beta}{\eta + 1} \frac{\rho^{\eta+1}}{\rho_0^{\eta}} + \frac{g_{sur}}{2\rho_0} (\nabla\rho)^2 \\ & + \frac{g_{sur,iso}}{\rho_0} (\nabla(\rho_n - \rho_p))^2 \\ & + \frac{C_s}{2} \left(\frac{\rho}{\rho_0}\right)^{\gamma_i} \delta^2 \rho + g_{\rho\tau} \frac{\rho^{8/3}}{\rho_0^{5/3}} \end{aligned} \quad (3)$$

Here,  $\delta$  is the isospin asymmetry.  $\delta = (\rho_n - \rho_p)/(\rho_n + \rho_p)$ ,  $\rho_n$  and  $\rho_p$  are the neutron and proton densities, respectively. A symmetry potential energy density of the form  $\frac{C_s}{2} \left(\frac{\rho}{\rho_0}\right)^{\gamma_i} \delta^2 \rho$  is used in the following calculations.

The energy density associated with the mean-field momentum dependence is represented by

$$u_{md} = \frac{1}{2\rho_0} \sum_{N_1, N_2} \frac{1}{16\pi^6} \int d^3p_1 d^3p_2 f_{N_1}(\vec{p}_1) f_{N_2}(\vec{p}_2) 1.57[\ln(1 + 5 \times 10^{-4}(\Delta p)^2)]^2. \quad (4)$$

where  $f_N$  are nucleon Wigner functions,  $\Delta p = |\vec{p}_1 - \vec{p}_2|$ , the energy is in MeV and momenta are in MeV/c. The resulting interaction between wavepackets is described in Ref. [36]. In this work, the  $\alpha = -356\text{MeV}$ ,  $\beta = 303\text{MeV}$ ,  $\eta = 7/6$ , and  $g_{sur} = 19.47 \text{ MeV fm}^2$ ,  $g_{sur,iso} = -11.35 \text{ MeV fm}^2$ ,  $C_s = 35.19\text{MeV}$ , and  $g_{\rho\tau} = 0\text{MeV}$ . These calculations use isospin-dependent in-medium nucleon-nucleon scattering cross sections in the collision term and the treatment of Pauli blocking effect is described in [29, 10, 11]. Fragments are formed in QMD approaches due to the A-body correlation dynamics and these correlations can be mapped onto the asymptotic final fragments by using the cluster recognition methods, such as minimum spanning tree algorithm (MST) and so on[37, 38, 39]. In this work, the clusters are recognized by means of the isospin dependent cluster recognition method (iso-MST)[40] which is an extended version of MST method and refines the description on the yield of neutron-rich LCPs, especially for the neutron-rich reaction systems.

Figure 1 presents the time evolution of the density contour plots for typical event of reaction  $^{64}\text{Zn}+^{64}\text{Zn}$  at  $E_{beam}=35\text{MeV/nucleon}$  and  $b=4\text{fm}$ . The results are obtained with  $\gamma_i = 0.5$ . As shown in figure 1, the projectile and target touch around  $60\text{fm/c}$  and form a low density neck region through which the nucleons transfer between the projectile and target. The compressed region reaches highest compress density at  $110\text{fm/c}$ . The projectile and target separate after  $160\text{fm/c}$ , whereupon the low-density neck connecting them ruptures into fragments. Two excited residues then continue along their paths and emit lighter fragments. The fluctuations which automatically appears in the QMD type models lead the system breaks via different break-up modes, such as binary, ternary and multi-fragmentation break-up modes, as shown in the Figure 1 (f1), (f2) and (f3), with different probabilities. Since the different break-up modes obviously lead to different emission patterns as well as the different angular and rapidity distributions of light charged particles (LCPs) and fragments (for example, Figure 1 (f1-f3)), one can expect that the branching ratios of binary, ternary and multi-fragmentation break-up

modes directly influence final results on the shape of rapidity distribution of the yields of LCPs.

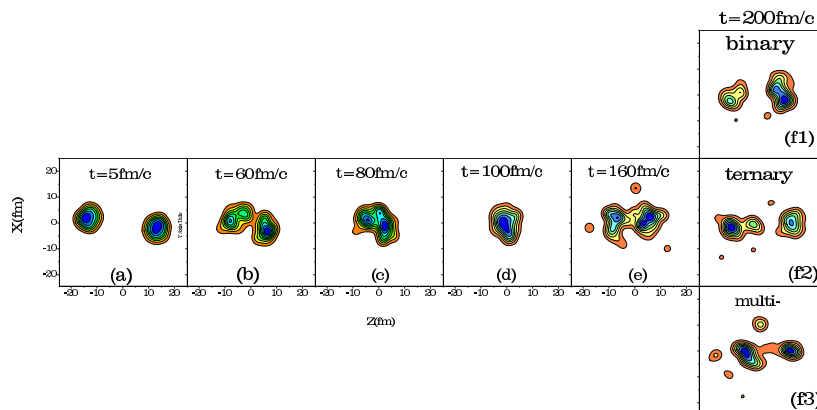


Figure 1: (Color online) Time evolution of the density contour plots for  $^{64}\text{Ni} + ^{64}\text{Ni}$  at  $E_{beam}=35$  MeV/nucleon for  $b=4$ fm from typical events which are calculated with  $\gamma_i = 0.5$ .

In Figure 2(a), we present the branching probability of different break-up modes for  $^{70}\text{Zn} + ^{70}\text{Zn}$  at  $E_{beam}=35$ MeV/nucleon and  $b=4$ fm with  $\gamma_i=2.0$  (solid symbols) and  $0.5$  (open symbols). The multi-fragmentation break-up mode is defined by  $M(Z \geq 3) \geq 4$  in this work, where  $M(Z \geq 3)$  is the multiplicity for fragments with  $Z \geq 3$ . The binary and ternary break-up modes mean the  $M(Z \geq 3)=2$  and  $M(Z \geq 3)=3$ , respectively. Our calculations with  $\gamma_i=2.0$  ( $\gamma_i=0.5$ ) show that  $\sim 18\%$  ( $\sim 19\%$ ) events for semi-peripheral  $^{70}\text{Zn} + ^{70}\text{Zn}$  collisions belong to binary mode,  $\sim 36\%$  ( $\sim 32\%$ ) events for ternary mode. The rest, almost  $\sim 46\%$  ( $\sim 49\%$ ) of total events, belong to the multi-fragmentation break-up mode as shown in Figure 2(b). Similar behaviors can be observed for  $^{64}\text{Zn}$  and  $^{64}\text{Ni}$  system. The values of the probability for  $M(Z \geq 3) \geq 4$  slightly depend on the mass of reaction system, those for  $^{70}\text{Zn}$  are the largest for both symmetry energy cases.

To understand the correlations between the break-up modes and LCPs emissions, we plot the rapidity distributions for the yields of LCPs corresponding to three kinds of break-up modes, binary (square symbols), ternary (circle symbols) and multi-fragmentation (triangle symbols) in Figure 3. Fig. 3 (a) and (b) are for neutron-poor particle,  $Y(^3\text{He})$ , (c) and (d) are for neutron-rich particles,  $Y(^6\text{He})$ . Left panels are for  $\gamma_i=2.0$  and right panels are for  $\gamma_i=0.5$ . The rapidity distributions for the yields of  $^3,^6\text{He}$  are normalized

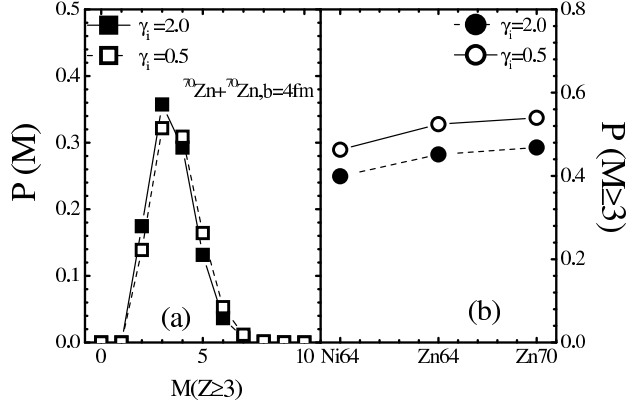


Figure 2: (Color online) (a) The calculated results on possibility distribution of multiplicity for fragments with  $Z \geq 3$  ( $M(Z \geq 3)$ ) for  $^{70}\text{Zn} + ^{70}\text{Zn}$  at  $E_{beam}=35$  MeV/nucleon and  $b=4\text{fm}$ , with  $\gamma_i = 2.0$  (solid symbols) and 0.5 (open symbols); (b) The possibilities of multi-fragmentation modes for  $^{70}\text{Zn} + ^{70}\text{Zn}$ ,  $^{64}\text{Zn} + ^{64}\text{Zn}$  and  $^{64}\text{Ni} + ^{64}\text{Ni}$  are for  $\gamma_i = 2.0$  (solid symbols) and 0.5 (open symbols).

to per event. It is clear that the binary and ternary modes tend to produce more  $^3\text{He}$  and  $^6\text{He}$  at midrapidity than that multi-fragmentation break-up mode does. The difference of  $Y(^6\text{He})$  between the binary, ternary modes and multi-fragmentation break-up mode is larger due to stronger isospin migration compared with that for  $Y(^3\text{He})$ . For example, for  $\gamma_i=2.0$ , the yield of  $^3\text{He}$  at  $y_r \sim 0$  from binary mode is 35% larger than that from multi-fragmentation mode, but the yield of  $^6\text{He}$  at  $y_r \sim 0$  from binary mode is 70% larger than that from multi-fragmentation break-up mode. Consequently, one can expect that the different break up modes lead to different shape of rapidity distribution of LCPs. The values of  $R_{yield}^{mid}$ , which is defined by the yield ratio between the mid-rapidity and projectile rapidity,

$$R_{yield}^{mid} = \frac{2 \cdot Y(0.0 \leq y_r \leq 0.5)}{Y(0.5 \leq y_r \leq 1.5)} \quad (5)$$

can quantitatively reflect the shape of rapidity distribution of the yields of LCPs, i.e.  $Y(y_r)/Y(y_r = 0)$ , as well as the degree of the preference of mid-rapidity emission for LCPs [24]. Based on above definition, one expects  $R_{yield}^{mid} > 1$  if there is a preference for emission around the middle rapidity. The narrower the shape of rapidity distribution of the normalized yield of LCPs is, the larger the  $R_{yield}^{mid}$  is. As results, the  $R_{yield}^{mid}$  values obtained with binary break-up mode are larger than that with multifragmentation break-

up mode, especially for the neutron-rich LCPs in dynamical approaches. For example, the value of  $R_{yield}^{mid}({}^6He)$  is 2.9 in binary break-up mode events, 2.5 in ternary break-up mode events and 2.4 in multi-fragmentation break-up mode events calculated with  $\gamma_i=2.0$ . This relationship between the  $R_{yield}^{mid}$  values and break-up modes is also valid for  $\gamma_i=0.5$ , but their absolute values are different. The  $R_{yield}^{mid}({}^6He)$  obtained with  $\gamma_i=0.5$  is 2.1 in binary break-up mode events, 1.8 in ternary break-up mode events and 1.8 in multi-fragmentation break-up mode events.

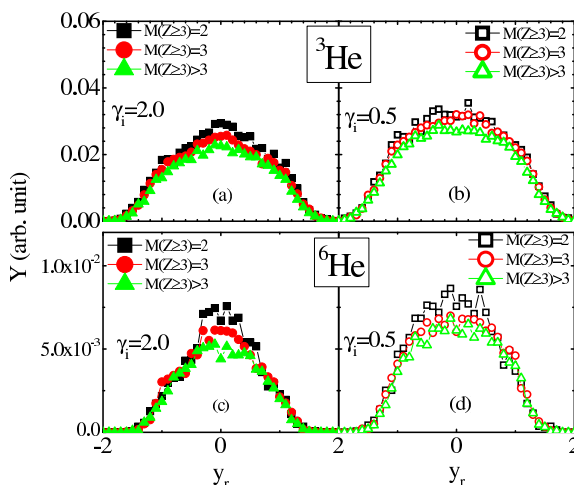


Figure 3: (Color online) (a) and (b) are the reduced rapidity ( $y_r$ ) distribution for the yield of  ${}^3He$ ,  $Y({}^3He)$ , with binary (square symbols), ternary (circle symbols) and multi-fragmentation (triangle symbols) break-up modes. (c) and (d) are for  $Y({}^6He)$ . (a) and (c) are the results with  $\gamma_i = 2.0$ , (b) and (d) are for  $\gamma_i = 0.5$ . All of those results are for  ${}^{70}Zn + {}^{70}Zn$  at  $E_{beam} = 35$  MeV/nucleon for  $b = 4$  fm.

Now, let's compare the calculated results of  $Y(y_r)/Y(y_r = 0)$  to the experimental data[24]. 100,000 events are performed for each reaction at different impact parameters. As an example, we present the  $Y(y_r)/Y(y_r = 0)$  for p, d, t,  ${}^3He$ ,  ${}^4He$  and  ${}^6He$ , for neutron-rich system  ${}^{70}Zn + {}^{70}Zn$  at  $b = 1, 6$  and  $8$  fm with  $\gamma_i = 2.0$  in Figure 4. Our calculations show that there is no strong dependence on the impact parameters in the range of experimental centrality  $b/b_{max} \cong 0.33 - 0.66$ [24], i.e.  $b \cong 3-6$  fm. Since the published data of  $Y(y_r)/Y(y_r = 0)$  [24] is for  ${}^{64}Ni + {}^{64}Ni$ , we only plot the  $Y(y_r)/Y(y_r = 0)$  for p, d, t,  ${}^3He$ ,  ${}^4He$  and  ${}^6He$ , for  ${}^{64}Ni + {}^{64}Ni$  at  $b = 4$  fm with  $\gamma_i = 0.5$  (open circles) and  $\gamma_i = 2.0$  (solid circles) in Figure 5 to get the physics insights. The data is plotted as stars[24]. Both our calculations and data show that the width of

distribution decreases with the mass of LCP increasing, because the Fermi motion of nucleons has larger impacts on the motion of lighter LCPs than that on heavier LCPs. Both theoretical and experimental results also clearly show that the width of  ${}^3\text{He}$  is smaller than that of  ${}^3\text{H}$  due to the isospin migration effects. Since the reaction systems calculated with  $\gamma_i=0.5$  produce larger probabilities of multi-fragmentation mode, and break up into more LCPs over the whole rapidity region than that with  $\gamma_i=2.0$ , the  $Y(y_r)/Y(y_r=0)$  for LCPs calculated with  $\gamma_i=0.5$  are wider than that with  $\gamma_i=2.0$ , especially for neutron rich LCPs. By comparing the simulated results to the data, one can find that the ImQMD05 calculations with stiffer symmetry energy case can well reproduce the data at forward rapidity region ( $y_r > 0$ ) for all p, d, t,  ${}^3\text{He}$ ,  ${}^4\text{He}$  and  ${}^6\text{He}$  particles. It suggests that branching probabilities for multi-fragmentation break-up modes should be around  $\sim 46\%$  for  ${}^{64}\text{Ni}+{}^{64}\text{Ni}$  as gained in this work. For the backward rapidity region ( $y_r < 0$ ), the obvious difference between the calculated results and the data is caused by lacking the efficiency for detection of LCPs at the backward [24] in calculation.

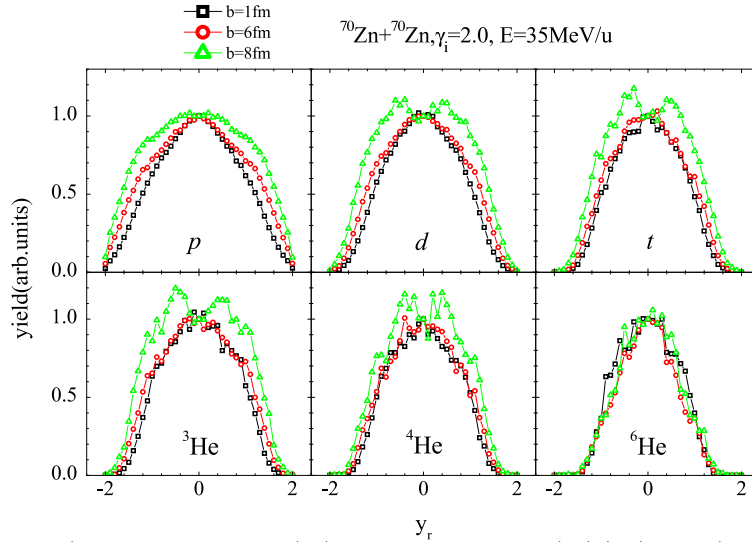


Figure 4: (Color online) Reduced rapidity ( $y_r$ ) distribution for  $Y(y_r)/Y(y_r=0)$ , for p, d, t,  ${}^3\text{He}$ ,  ${}^4\text{He}$  and  ${}^6\text{He}$  for  ${}^{70}\text{Zn} + {}^{70}\text{Zn}$  at impact parameter  $b=1, 6, 8\text{fm}$ . The calculations are obtained with  $\gamma_i=2.0$

In order to quantitatively understand the influence of the density dependence of symmetry energy and sequential decay on the shape of rapidity distribution of yields for LCPs, we investigate the  $R_{yield}^{mid}$  values of the LCPs as a function of the product of charge and mass ( $AZ=1$  for  ${}^1\text{H}$ ,  $AZ=2$  for  ${}^2\text{H}$ ,

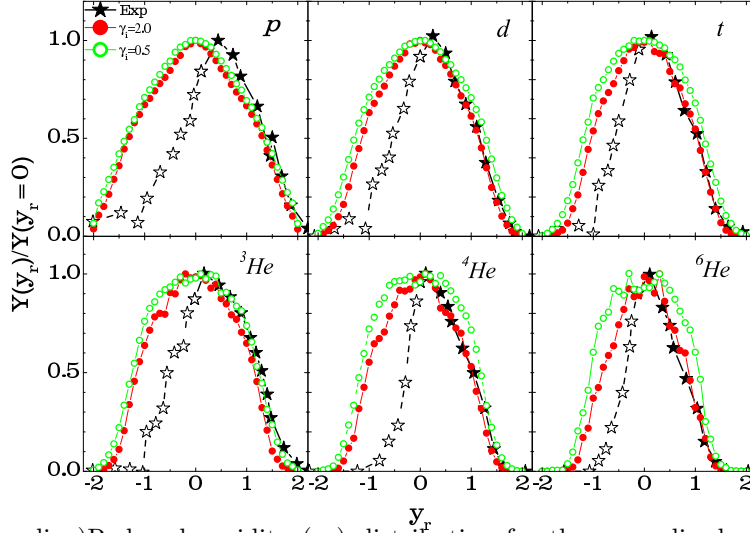


Figure 5: (Color online) Reduced rapidity ( $y_r$ ) distribution for the normalized yields of  $p$ ,  $d$ ,  $t$ ,  ${}^3\text{He}$ ,  ${}^4\text{He}$  and  ${}^6\text{He}$ , i.e.  $Y(y_r)/Y(y_r = 0)$ , for  ${}^{64}\text{Ni} + {}^{64}\text{Ni}$  at 35MeV/nucleon and  $b=4\text{fm}$ . The experimental data is shown as the stars. The ImQMD05 calculation for  $\gamma_i = 0.5$  is shown as the open circles and the solid circles are for  $\gamma_i = 2.0$ . Each distribution is normalized with its yield at  $y_r = 0$ .

AZ=3 for  ${}^3\text{H}$ , AZ=6 for  ${}^3\text{He}$ , AZ=8 for  ${}^4\text{He}$  and AZ=12 for  ${}^6\text{He}$ ) for three reaction systems  ${}^{64}\text{Zn} + {}^{64}\text{Zn}$ ,  ${}^{64}\text{Ni} + {}^{64}\text{Ni}$  and  ${}^{70}\text{Zn} + {}^{70}\text{Zn}$ . A series calculations with different density dependence of symmetry potential, i.e.  $\gamma_i=0.5, 0.75, 1.0, 2.0$  at  $b=4\text{fm}$  are performed. As shown in Fig.6, the ImQMD05 calculations can reasonably reproduce the data of  $R_{\text{yield}}^{\text{mid}}$  as a function of AZ for  ${}^{64}\text{Zn} + {}^{64}\text{Zn}$ , and qualitatively reproduce the trends of  $R_{\text{yield}}^{\text{mid}}$  for neutron-rich reaction systems  ${}^{64}\text{Ni} + {}^{64}\text{Ni}$  and  ${}^{70}\text{Zn} + {}^{70}\text{Zn}$ . The calculated results show the values of  $R_{\text{yield}}^{\text{mid}}$  for neutron-rich isotopes, such as  ${}^6\text{He}$ , clearly depend on the density dependence of symmetry energy. Since the calculations with stiffer symmetry energy have stronger isospin migration effects and predict smaller probabilities of multi-fragmentation mode, it predicts larger  $R_{\text{yield}}^{\text{mid}}$  values. The calculations with symmetry energy ( $\gamma_i \geq 0.75$ ) reasonably reproduce the data of  $R_{\text{yield}}^{\text{mid}}$  as a function of AZ for  ${}^{64}\text{Zn} + {}^{64}\text{Zn}$ . But for the neutron-rich reaction systems  ${}^{64}\text{Ni} + {}^{64}\text{Ni}$  and  ${}^{70}\text{Zn} + {}^{70}\text{Zn}$ , calculated results of  $R_{\text{yield}}^{\text{mid}}$  for  ${}^6\text{He}$  are obviously smaller than the data whatever the form of symmetry energy is used in the model. The possible reason is that the probabilities of binary and ternary break-up modes in neutron-rich reaction systems are underestimated in the QMD approaches than observed in experiments, especially for

neutron rich systems. It may be caused by lacking the fine structure effects of neutron-rich nuclei (such as neutron skin, stability of lighter neutron-rich nuclei) which may become more and more important with the beam energy decreasing in HICs simulations. Since the secondary decay also plays important roles on the yields of LCPs, such as p, d, t,  $^3\text{He}$ ,  $^4\text{He}$  and  $^6\text{He}$ , and thus it may influence the ratio observables, such as  $Y(y_r)/Y(y_r = 0)$  and  $R_{yield}^{mid}$ . We have simulated decays of fragments created in the collisions using the GEMINI code [41] to examine the influence of sequential decays. Sequential decays enhance the yields of LCPs, but such effects are largely suppressed in the ratio observables,  $Y(y_r)/Y(y_r = 0)$  and  $R_{yield}^{mid}$  except for  $^4\text{He}$ . However, the exact effects after coupling the sequential decay to transport codes need to be further explored in the future.

Moreover, the behaviors of  $R_{yield}^{mid}$  as a function of AZ for He elements are different from the SMF predictions (left triangles in Fig.6) in which a weakly AZ dependence of the  $R_{yield}^{mid}$  for He isotopes was obtained [24]. The possible reasons are: many-body correlations in the QMD models cause large fluctuation, and it enhances the probability of multi-fragmentation break-up modes, and produces copious fragments and light particles over the whole rapidity region in the QMD simulations. Fast fragmentation dynamics inhibits nucleon exchanging and charge equilibration due to the many-body correlations and strict Pauli blocking. As a consequence, the neutron-rich He tend to locate at mid-rapidity than neutron-poor LCPs, and thus, the larger the isospin asymmetry of He is, the larger the  $R_{yield}^{mid}$  is.

In summary, we have studied the LCPs emissions in three reaction systems  $^{70}\text{Zn}+^{70}\text{Zn}$ ,  $^{64}\text{Zn}+^{64}\text{Zn}$  and  $^{64}\text{Ni}+^{64}\text{Ni}$  at the beam energy of 35MeV/nucleon and  $b=4\text{fm}$  to explore the fragmentation mechanism and relationship between the break-up modes and rapidity distribution of LCPs with ImQMD05. Our studies show there is interplay between the binary, ternary and multi-fragmentation break-up modes. The binary and ternary break-up modes more prefer to produce LCPs at mid-rapidity, and it leads to a narrower reduced rapidity distribution for the yield of LCPs than the multi-fragmentation break-up mode does. Based on the correlations between the fragmentation mode and LCPs emissions, one can estimate the probability of multi-fragmentation break-up modes by studying the reduced rapidity distribution for the normalized yields of p, d, t,  $^3\text{He}$ ,  $^4\text{He}$  and  $^6\text{He}$  and the corresponding values of  $R_{yield}^{mid}$ . Current analysis suggests that reproducing the data of  $Y(y_r)/Y(y_r = 0)$  for p, d, t,  $^3\text{He}$ ,  $^4\text{He}$  and  $^6\text{He}$  and corresponding  $R_{yield}^{mid}$  in theory requires that  $\geq 40\%$  of the collisions events belong to the

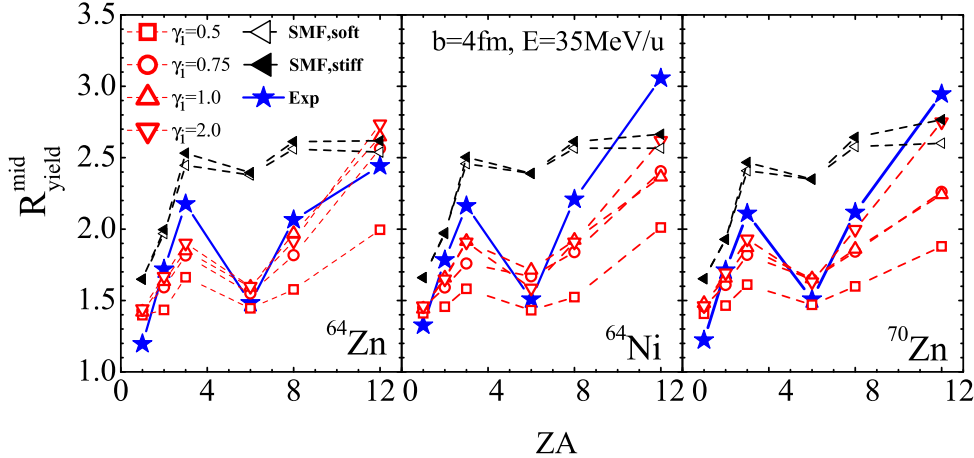


Figure 6: (Color online)  $R_{yield}^{mid}$  values as a function of the charge times mass ( $ZA$ ) for  $p$  ( $ZA=1$ ),  $d$  ( $ZA=2$ ),  $t$  ( $ZA=3$ ),  ${}^3He$  ( $ZA=6$ ),  ${}^4He$  ( $ZA=8$ ),  ${}^6He$  ( $ZA=12$ ). The open symbols are the results obtained with ImQMD05 for  $\gamma_i = 0.5, 0.75, 1.0$  and  $2.0$ . Left triangles are the results from SMF calculations and the solid stars are the data from [24].

multi-fragmentation break-up mode in dynamical approaches. This values could also be slightly modified after including the tensor force and spin-orbit interaction, which were found to influence the dissipation dynamics at lower energy[43], in transport model. Furthermore, experimental measurements/reanalysis on the correlation between the probability of multi-fragmentation break-up mode and  $R_{yield}^{mid}$  would give more comprehensive information on the reaction mechanism, and it will be also helpful for tightly constraining the symmetry energy with HICs in the future.

**Acknowledgements** Yingxun Zhang thanks the Prof. M.Colonna on helpful communications. This work has been supported by Chinese National Science Foundation under Grants (11475262,11422548,11375062,11375094), the 973 program of China No. 2013CB834404.

## References

- [1] Bondorf J P, Botvina A S, Iljinov A S, Mishustin I N, and Sneppen K. Statistical multifragmentation of nuclei. Phys. Rep. 1995, 257: 133–221
- [2] Gross D H E. Statistical decay of very hot nuclei-the production of large clusters. Rep. Prog. Phys.1990, 53: 605–
- [3] Das C B, Gupta S Das, Lynch W G, Mekjian A Z, Tsang M B. The thermodynamic model for nuclear multifragmentation. Phys.Rep.2005, 406: 1-47

- [4] Souza S R, Tan W P, Donangelo R, Gelbke C K, Lynch W G, and Tsang M B. Nuclear isotope thermometry. *Phys. Rev. C*2000, 62: 064607
- [5] D'Agostino M, Botvina A S, Milazzo P M, et al. Statistical multifragmentation in central Au + Au collisions at 35 MeV/u. *Phys. Lett. B*1996, 371: 175
- [6] Williams C, Lynch W G, Schwarz C, et al. Fragment distributions for highly charged systems. *Phys. Rev. C*1997, 55: R2132–
- [7] Ogul R, Botvina A S, Atav U, et al. Isospin-dependent multifragmentation of relativistic projectiles. *Phys.Rev.C* 2011,83: 024608–
- [8] Aichelin J. Quantum molecular dynamicsa dynamical microscopic n-body approach to investigate fragment formation and the nuclear equation of state in heavy ion collisions. *Phys. Rep.*1991, 202: 233
- [9] Hartnack C, et al. Modelling the many-body dynamics of heavy ion collisions: Present status and future perspective. *Eur. Phys. J. A* 1, 151 (1998).
- [10] Zhang Yingxun and Li Zhuxia. Elliptic flow and system size dependence of transition energies at intermediate energies. *Phys. Rev. C*2006, 74: 014602
- [11] Zhang Yingxun, Li Zhuxia, and Danielewicz P. In-medium NN cross sections determined from the nuclear stopping and collective flow in heavy-ion collisions at intermediate energies. *Phys. Rev. C*2007, 75: 034615
- [12] Le Fevre A and Aichelin J. Bimodality: A Sign of Critical Behavior in Nuclear Reactions. *Phys.Rev.Lett.*2008, 100: 042701
- [13] Amorini F, Cardella G, Giuliani G, et al. Isospin Dependence of Incomplete Fusion Reactions at 25MeV/Nucleon. *Phys.Rev.Lett.*2009, 102: 112701
- [14] Cardella G, Giuliani G, Lombardo I, et al. Effects of neutron richness on the behavior of nuclear systems at intermediate energies. *Phys. Rev. C*2012, 85: 064609

- [15] Li Zhuxia, Hartnack C, Stocker H and Greiner W. Transition from binary processes to multifragmentation in quantum molecular dynamics for intermediate energy heavy ion collisions. *Phys.Rev.C*44, 824(1991).
- [16] Tian Junlong, Wu Xizhen, Zhao Kai, Zhang Yingxun. Properties of the composite systems formed in the reactions of U238+U238 and Th232+Cf250. *Phys. Rev. C*2008, 77: 064603
- [17] De Filippo E, Pagano A, Wilczynski J, et al. Time sequence and time scale of intermediate mass fragment emission. *Phys.Rev.C*2005, 71: 044602
- [18] Hudan S, McIntosh A B, de Souza R T, et al. Tracking saddle-to-scission dynamics using N/Z in projectile breakup reactions. *Phys.Rev.C*2012, 86: 021603(R)
- [19] McIntosh A B, Hudan S, Black J, et al. Short-lived binary splits of an excited projectile-like fragment induced by transient deformation. *Phys.Rev.C*2010, 81: 034603
- [20] Wang R S, Zhang Y, Xiao Z G, Tian J L, Zhang Y X, Wu Q H, Duan L M, et al. Time-dependent isospin composition of particles emitted in fission events following Ar40+Au197 at 35 MeV/u. *Phys.Rev.C*2014, 89:064613
- [21] Wu Qianghua, Zhang Yingxun, Xiao Zhigang, Wang Rensheng, Zhang Yan, et al. Competition between Coulomb and symmetry potential in semi-peripheral heavy ion collisions. *Phys.Rev.C*91,014617(2015)
- [22] Souliots G A, Veselsky M, Chubarian G, et al. Enhanced Production of Neutron-Rich Rare Isotopes in Peripheral Collisions at Fermi Energies. *Phys. Rev. Lett.*2003, 91: 022701
- [23] Souliots G A, Veselsky M, Yennello S J. Heavy-residue isoscaling as a probe of the process of N/Z equilibration. *Phys. Lett. B*2004, 588:35
- [24] Kohley Z, May L W, Wuenschel S, et al. Transverse collective flow and midrapidity emission of isotopically identified light charged particles. *Phys.Rev.C*2011, 83: 044601

- [25] Kohley Z, Bonasera A, Galanopoulos S, et al. Correlations with projectile-like fragments and emission order of light charged particles. *Phys.Rev.C*86, 044605(2012).
- [26] Baran V, Colonna M, Di Toro M, et al. Isospin transport at Fermi energies. *Phys.Rev.C*2005, 72: 064620
- [27] Baran V, Colonna M, Di Toro M. Neck fragmentation reaction mechanism. *Nucl.Phys.A*2004, 730:329
- [28] Rizzo J, et al. Isospin dynamics in peripheral heavy ion collisions at Fermi energies. *Nucl. Phys. A*2008, 806: 79
- [29] Zhang Yingxun and Li Zhuxia. Probing the density dependence of the symmetry potential with peripheral heavy-ion collisions. *Phys. Rev. C*2005, 71: 024604
- [30] Colonna M, Baran V, Di Toro M, Frecus B, and Zhang Yingxun. Reaction mechanisms in transport theories: a test of the nuclear effective interaction. *Journal of Physics: Conference Series*2013, 420:012104
- [31] Zhang Yingxun, Li Zhuxia, Zhou Chengshuang, Chen Jixian, Colonna M, Danielewicz P, Tsang M B. Probing the symmetry energy with isospin ratio from nucleons to fragments. *Journal of Physics: Conference Series*2013, 420: 012106
- [32] De Filippo E, Pagano A, Russotto P, et al. Correlations between emission timescale of fragments and isospin dynamics in  $^{124}\text{Sn}+^{64}\text{Ni}$  and  $^{112}\text{Sn}+^{58}\text{Ni}$  reactions at 35A MeV. *Phys. Rev. C*2012, 86: 014610
- [33] Fan Xiaohua, Dong Jianmin, Zuo Wei. Symmetry energy at subsaturation densities and the neutron skin thickness of  $^{208}\text{Pb}$ . *Sci China-Phys Mech Astron*, 2015, 58(6): 062002
- [34] Mo Qihong, Liu Min, Chen LiChun, et al. Deformation dependence of symmetry energy coefficient of nuclei. *Sci China-Phys Mech Astron*, 2015, 58(8): 082001
- [35] Qu Xiaoying, Chen Ying, Zhang Shuangquan, et al. Extending the nuclear chart by continuum: From Oxygen to titanium. *Sci China-Phys Mech Astron*, 2013, 56(11):2031–2036.

- [36] Aichelin J, Rosenhauer A, Peilert G, Stocker H and Greiner W. Importance of Momentum-Dependent Interactions for the Extraction of the Nuclear Equation of State from High-Energy Heavy-Ion Collisions. *Phys. Rev. Lett.*1987, 58: 1926
- [37] Dorso C O and Randrup J. Early recognition of clusters in molecular dynamics. *Phys. Lett. B*1993, 301: 328
- [38] Puri R K and Aichelin J. Simulated Annealing Clusterization Algorithm for Studying the Multifragmentation. *J. Comput. Phys.*2000, 162: 245
- [39] Goyal S and Puri R K. Formation of fragments in heavy-ion collisions using a modified clusterization method. *Phys. Rev. C*2011, 83: 047601
- [40] Zhang Yingxun, Li Zhuxia, Zhou Chengshuang, Tsang M B. Effect of isospin-dependent cluster recognition on the observables in heavy ion collisions. *Phys.Rev.C*2012, 85: 051602(R)
- [41] Charity R J, et al. Systematics of complex fragment emission in niobium-induced reactions. *Nucl. Phys. A*1988, 483: 371
- [42] Tsang M B, Bougault R, Charity R, et al. Comparisons of statistical multifragmentation and evaporation models for heavy-ion collisions. *Eur. Phys. J. A*2006, 30:129; 2007, 32: 243
- [43] Dai Gaofeng, Guo Lu, Zhao Enguang, Zhou Shangui. Effect of tensor force on dissipation dynamics in time-dependent Hartree-Fock theory. *Sci China-Phys Mech Astron*, 2014, 57(9):1618–1622.